SEISMIC BEHAVIOUR OF UNREINFORCED MASONRY WALLS

M. J. N. Priestley*

ABSTRACT

The behaviour of unreinforced masonry walls under seismic loading is considered, with particular emphasis being given to face-load response. It is shown that traditional methods of assessing seismic performance based on elastic stress calculations result in excessively conservative results when compared with more realistic methods of assessment. In particular, an assessment procedure based on energy considerations is developed at some length, and is illustrated by a worked sample.

INTRODUCTION

Ultimate strength methods of design and analysis are now accepted in New Zealand as necessary for assessing performance of reinforced masonry structures under seismic loading[1] and are required by the provisonal masonry design code[2]. However, when assessing the strength of existing unreinforced buildings, it is still common to use elastic analysis techniques to specified stress levels. It will be shown shortly that even for non-seismic applications working stress methods are inappropriate, and that ultimate strength methods produce more consistent results. When considering seismic loading, these considerations become even more important. However, simple ultimate strength calculations still do not necessarily adequately predict the behaviour of unreinforced masonry, any more than they do for reinforced concrete or masonry structures under seismic loading. For these latter materials, a further consideration, that of ductility, is necessary to reconcile the satisfactory performance of structures designed for strength levels only a fraction of that corresponding to elastic response to the design level earthquake.

For unreinforced masonry structures, it would initially appear that ductility considerations are inappropriate, since ductility is normally provided in structures primarily by inelastic straining of steel, either in the form of reinforcing bars or structural steel sections. However, the concept of ductility is based on energy considerations, and it can be shown that if these considerations are applied to the analysis of unreinforced masonry, the level of seismic loading required to cause failure, particularly for face-loaded walls, tends to greatly exceed that predicted by simple ultimate strength calculations.

This contention is supported by results from an extensive U.S. research programme examining the seismic performance of unreinforced masonry, reported by Kariotis et al.[3,4]. Extensive dynamic analyses and shake-table testing of face-loaded walls indicated that the walls could sustain levels of excitation acceleration far greater than that predicted by elastic or ultimate strength calculations. Similar results have been obtained from limited testing of masonry veneers[5]. Kariotis et al. found that a correlation could be found between the strength of face-loaded walls and the spectral velocity of the input acceleration, which indicates that energy considerations are important.

The work described in this paper is an attempt to explain the behaviour described by Kariotis et al. by the use of simple fundamental analytical methods that might be suitable for the design office.

COMPARISON BETWEEN ELASTIC AND ULTIMATE STRENGTH METHODS

Elastic design puts undue emphasis on masonry stress levels. In fact, stress levels are rather insignificant for unreinforced masonry, and seismic capacity is likely to be governed not by material strength, but by stability and energy considerations, as asserted in the Introduction to this paper. Even for more simple lateral load cases, such as wind loading, elastic design to specified stress levels is inappropriate, as shown by the example of Fig. 1 and 2. In Fig. 1a and 1b a typical four-storey shear wall is subjected to floor loads P_1 to P_4 and lateral loads H_1 to H_4, resulting in a total axial force P_e and moment M_e at the wall base. Typically axial compression stresses under P_e will be light, and the maximum moment permitted by elastic design will depend on the maximum allowable tension stress f_t. Many codes allow masonry tension stresses under elastic design. The maximum moment for elastic design will thus be

$$M_e \leq \left(\frac{P_e}{\ell_w t} + f_t\right) \frac{\ell_w^2 t}{6} \qquad (1)$$

*Reader in Civil Engineering,
University of Canterbury, Christchurch
New Zealand

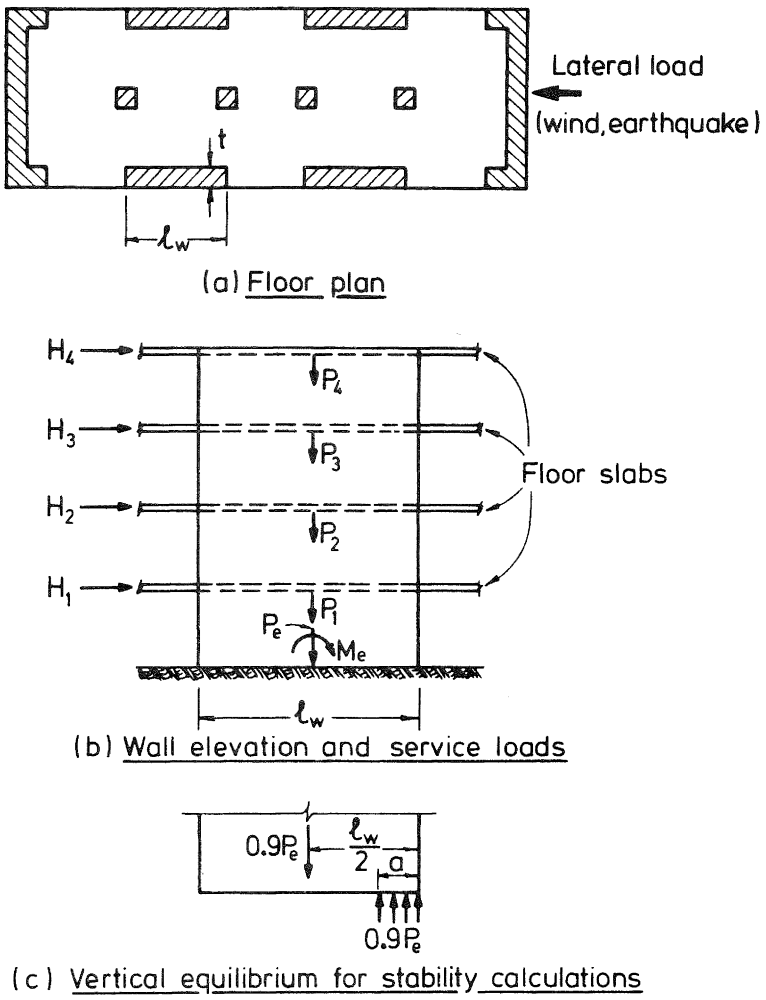

Figure 1. Unreinforced masonry wall under wind loading.

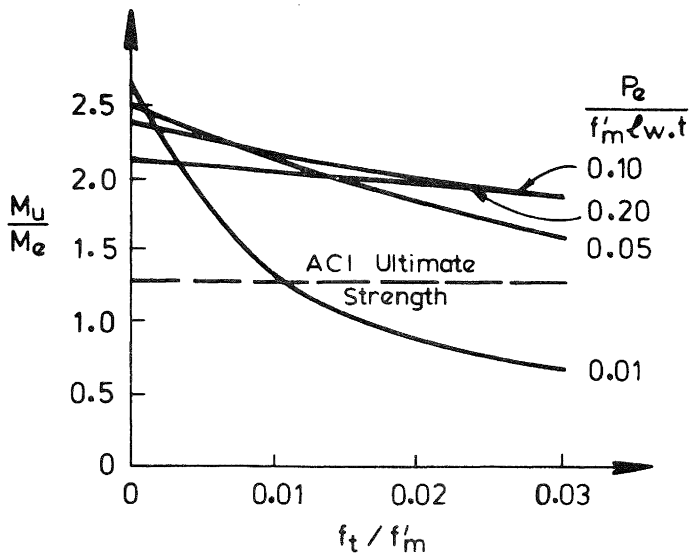

Figure 2. Comparison between elastic and ultimate moment capacities for unreinforced masonry wall.

where ℓ_w and t are the wall length and thickness respectively at the base.

For ultimate strength calculations it would be normal to check the moment capacity under reduced gravity load. Figure 1c shows forces involved in vertical equilibrium under an ultimate stability state defined by

$$U = 0.9D + 1.3W \quad (2)$$

which is commonly used for ultimate strength design wind loading[6,7]. Assuming an average uniform compression stress of $0.85f'_m$ at the toe, and noting that cracking is assumed to have occurred, the length of the compression zone, a, is given by

$$a = \frac{0.9\ P_e}{0.85\ f'_m t} \quad (3)$$

and the ultimate moment capacity by

$$M_u = 0.9\ P_e\ (\frac{\ell_w - a}{2}) \quad (4)$$

Figure 2 compares the ratio of ultimate moment (Eqn. (4)) to design elastic moment (Eqn. (1)) for a range of axial load levels $P_e/f'_m \ell_w t$ and allowable tension strength f_t/f'_m. It will be seen that the level of protection against overturning afforded by elastic theory is inconsistent, but is generally very conservative compared with typical ultimate strength design. However, for very low axial load levels, elastic theory may produce unconservative results, as shown by the curve for $P_e/f'_m \ell_w t = 0.01$ in Fig. 2.

The maximum lateral wind loads that the wall can sustain are limited by the ultimate moment capacity given by Eqn. 4. Any attempt to subject the building to higher wind loads would result in collapse by overturning. However, for seismic loading, the development of ultimate moment capacity, and incipient rocking about a wall toe does not represent failure. The seismic lateral forces are related to ground acceleration and wall stiffness. Once the wall starts to rock its incremental stiffness becomes zero, and any increase in ground acceleration will not increase forces on the wall. Failure can only occur by overturning if the acceleration pulse inducing rocking continues with the same sign for sufficient length of time to induce collapse. It is thus clear that collapse will be related to the seismic energy input. If the ground acceleration changes direction soon after rocking commences, the wall stabilises and rocking ceases. It will be shown later that the amount of energy required for overturning of typical masonry shear walls under in-plane loading is too high to result in failure, though face loading instability may cause collapse.

Unreinforced walls subjected to face-load excitation

The response of unreinforced masonry walls to out-of-plane (face-load) seismic excitation is one of the most complex and ill-understood areas of seismic analysis. Consider the simplified four-storey masonry building shown in Fig. 3 subjected to ground acceleration $\ddot{a}_g$ perpendicular to the two front walls, which are thus subjected to inertia loads in the weak, face-load direction. Although the base of one of these walls is subjected to the ground acceleration, the acceleration input to the walls at levels 1 to 4 is applied by the floor slabs, and will have quite different characteristics to the ground acceleration. The energy input path is shown by dashed lines in Fig. 3. Thus the end walls, acting as in-plane shear walls respond to the ground acceleration with response accelerations that depend on height, wall stiffness and contributory mass from the floors and face-loaded walls. The wall response accelerations at a given height act as input accelerations to the floor diaphragms. If these are rigid, the displacements and accelerations at all points along the floor will be equal to the end wall displacements and accelerations. However, if the floor is flexible, as will often be the case for existing masonry buildings, response displacements and accelerations may well be modified from the end-wall values. The floor diaphragm response in turn becomes the input acceleration for the face-loaded wall. The ground acceleration has thus been modified by two actions: that of the end shear walls and that of the floor diaphragms before acting as an input acceleration to the face-loaded wall.

The interactions implied by this behaviour are described schematically in Fig. 4. In order to fully investigate the interaction, three-dimensional dynamic analyses are necessary. However, these are generally too complex and costly to carry out for real structures. It should be noted that the consequence is that input accelerations to the face-loaded wall, at the different floor levels will be of different magnitude, and may be out of phase, or have significantly different frequency composition.

Figure 5 describes the response in terms of response spectra. Figure 5a shows the elastic response spectrum for the end shear wall response to the ground excitation. For the fundamental period of transverse response, T, the response acceleration $\ddot{a}_r$ can be calculated. It should be noted that the elastic response spectrum forms an upper bound to response, and a lower response acceleration will be appropriate if the wall rocks on its base at less than the elastic response acceleration.

The response acceleration $\ddot{a}_r$ refers to the acceleration at the effective centre of seismic force, h_e. On the assumption of a linear first mode shape, the peak response accelerations at the different levels can be calculated by linear

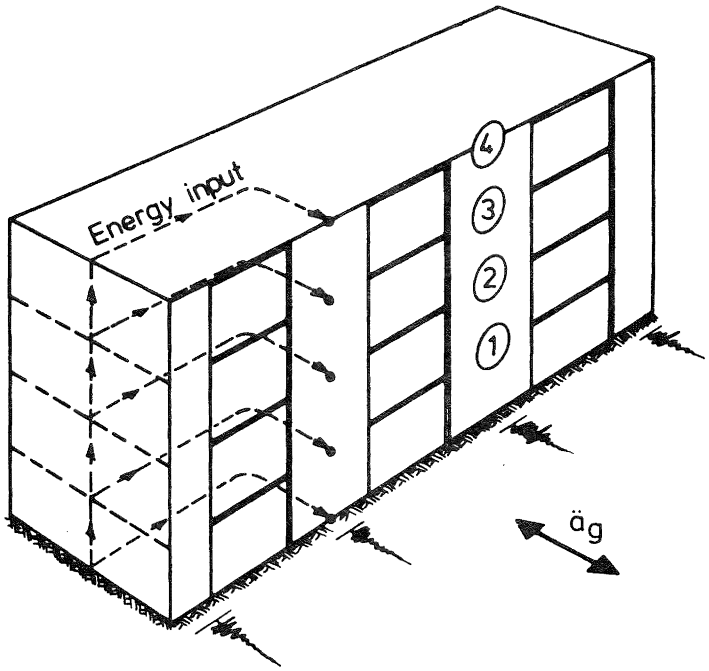

Figure 3. Seismic load path for unreinforced masonry building.

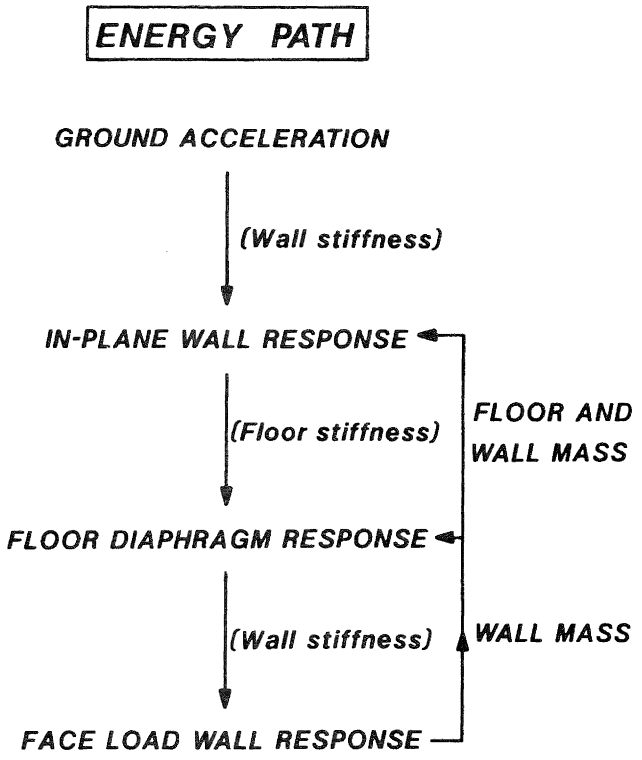

Figure 4. Seismic Energy Path.

extrapolation. However, it must be realised that these accelerations are accelerations relative to ground acceleration, and must have the ground acceleration added to represent total (absolute) acceleration. Thus, though the mode shape indicates zero acceleration at ground level, it is clear that the maximum absolute acceleration at this level is of course $\ddot{a}_g$, the peak ground acceleration.

At higher levels the peak absolute acceleration is less easy to define unless a full dynamic time-history computer analysis is carried out. It would be unrealistically conservative to add the peak ground acceleration to the peak response accelerations, since the two accelerations will not commonly occur simultaneously. In fact, in a resonant situation, the response and ground accelerations will be out of phase, and hence will subtract. Figure 5 illustrates an average compromise solution for estimating peak accelerations from a response spectrum approach. At heights above the centre of seismic force, h_e, the peak accelerations are given by the mode shape from the response accelerations. That is, ground accelerations, which are as likely to decrease as to increase the absolute acceleration, are ignored. At heights less than h_e, the increasing significance of the ground acceleration is acknowledged by use of a linear design acceleration envelope from $\ddot{a}_g$ at ground level to $\ddot{a}_r$ at h_e. An alternative, and somewhat more conservative approach would be to use a square-root-sum-of-the-square approach (SRSS). That is

$$\ddot{a}_{ai} = \sqrt{\ddot{a}_{ri}^2 + \ddot{a}_g^2} \qquad (5)$$

where $\ddot{a}_{ri}$ is the response spectrum modal acceleration at floor i, and $\ddot{a}_{ai}$ is the absolute maximum acceleration at floor i.

The floor accelerations in Fig. 5b, whether calculated by the linear or SRSS models described above, now become the input acceleration for floor response. Since the end-wall response will largely be comprised of energy at the natural period T of the transverse reponse, the response of the floor to the end wall excitation will depend on the ratio of the natural floor period T_f to the wall period T, and the equivalent viscous damping, as shown in Fig. 5c. For very stiff floors, ($T_f \fallingdotseq 0$) the response acceleration will be equal to the excitation acceleration. For very flexible floors, the response accelerations will be small, but for values of T_f/T_r close to 1.0, resonant response could occur, with high amplification of end wall response.

Figure 6 illustrates the resulting floor excitaton for face loading the wall, assuming all the floors amplify the end wall accelerations by an equal amount, and are in phase. Though this will be no means always be the case, it represents the worst case for face load excitation to the wall. In Fig. 6 it will be seen that the ground level excitation consists of a wide mix of frequency components, but at higher levels, the response consists of a dominant frequency: that of transverse response of the building as a whole dominated by the

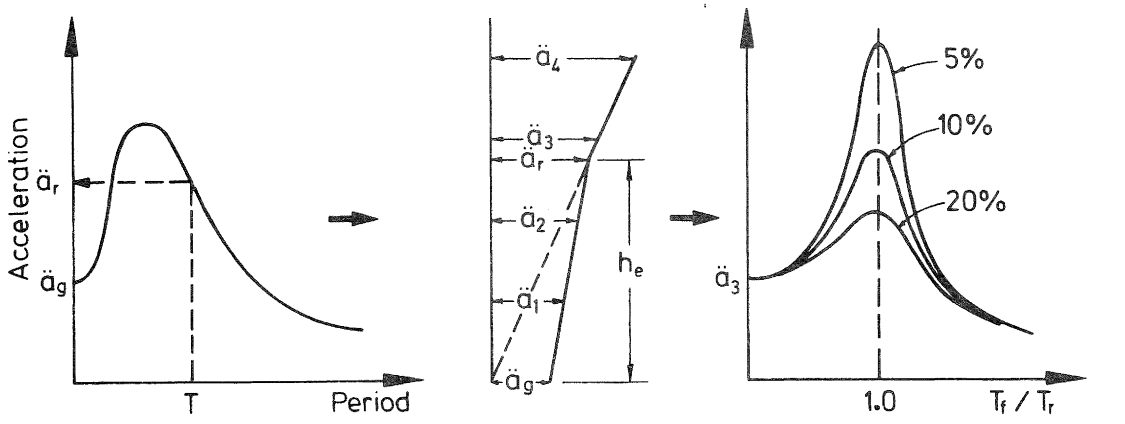

(a) Elastic response spectrum for end walls to ground excitation

(b) Variation of response acceleration with height

(c) Elastic response spectra for response of 3rd floor to end wall excitation

Figure 5. Flexible-floor response to ground excitation.

end wall stiffness. As indicated by Fig. 5b, the level of response acceleration increases with height. Consequently the top level floor is subjected to the maximum excitation accelerations. Since this is combined with the lowest axial load (and hence lowest stability moment capacity) failure of the wall is expected initially at the top level. This agrees with many cases of earthquake damage to unreinforced masonry buildings.

The final stage in the energy path for face load excitation is represented by Fig. 7 for one of the storeys of a multistorey unreinforced masonry building. Inertial response of the wall in face-loading is excited by the floor accelerations $\ddot{a}_i$ and $\ddot{a}_{i+1}$ below and above the wall. Although the response acceleration $\ddot{a}_{in}$ will vary with height up the wall, and will be a maximum at midheight, and minimum at the floor levels, it is not excessively conservative to assume $\ddot{a}_{in}$ to be constant with height, as indicated in Fig. 7a. The magnitude of $\ddot{a}_{in}$ depends again on the ratio of natural frequency of wall response to floor excitation frequency, indicated by the period ratio T_{in}/T_f, in Fig. 7b. If the wall responds elastically without cracking the response acceleration is comparatively easy to calculate. However, as the wall cracks, and commences to rock (as discussed shortly), the natural period will lengthen, changing the response amplification of input acceleration. This effect can be very hard to quantify. Fig. 7b shows two possibilities. With a moderate period shift from 1 to 2 in Fig. 7b, coupled with light damping, the face-load response of the wall will be effected by resonance, and be substantially higher than the input acceleration. For larger displacements, the equivalent period may shift past the resonant range to point 3 , resulting in lower response accelerations than input accelerations.

However, for the large displacements necessary to cause structural collapse, the response period will be quite long, and equivalent viscous damping quite high. It thus seems reasonable to assume that the response acceleration is the average of the input accelerations $\ddot{a}_i$ and $\ddot{a}_{i+1}$.

Conditions at failure and equivalent 'elastic' response

Figure 8 illustrates the conditions representing failure for a face-loaded wall element such as described in the previous section. The formation of cracking does not constitute wall failure, even in an unreinforced wall. Failure can only occur when the resultant compression force R in the compression zone of the central crack is displaced outside the line of action of the applied loads at top and bottom of the wall.

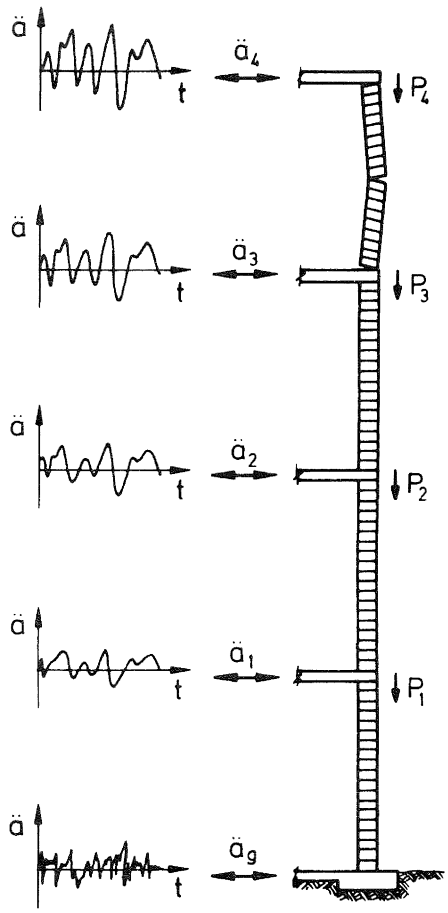

Figure 6. Face-load response of wall to floor accelarations.

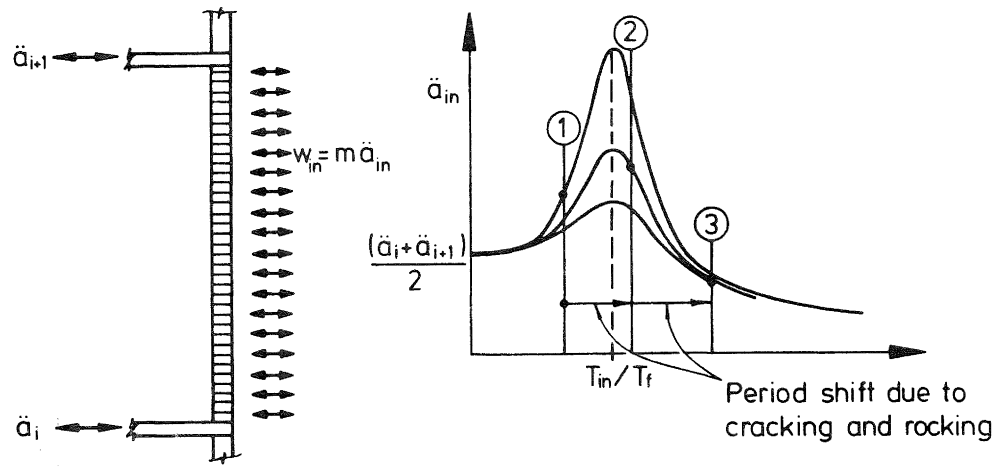

Figure 7. Inertia loads from face-load response.

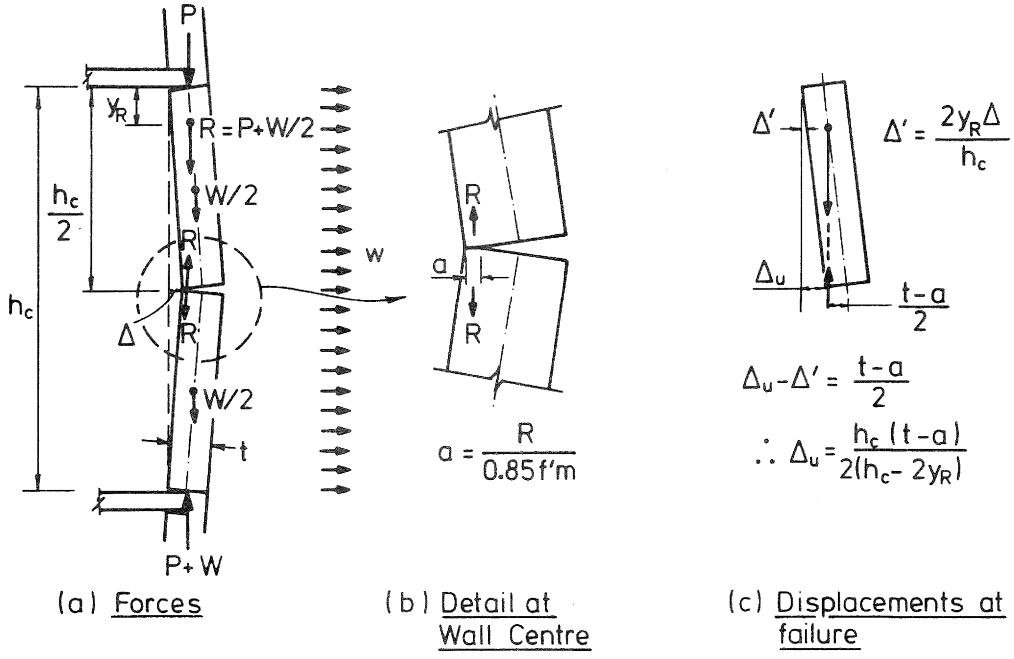

Figure 8. Conditions for failure of wall under face loading.

In developing the equations to predict conditions for wall failure, some simplifying assumptions are necessary. First, as mentioned above, it will be assumed that the response acceleration $\ddot{a}_{in}$ is constant up the wall height. Hence the lateral inertia force per unit area will be

$$w_{in} = m.\ddot{a}_{in} \qquad (6)$$

where m is the wall mass per unit area of wall surface. The second assumption concerned the degree of end fixity for the wall at floor levels. It is conservatively assumed that the ends are simply supported (i.e. no end moments). This would be appropriate if the walls at alternate storey heights were displacing out-of-phase by 180^o, which is a real possibility.

Figure 8a shows the forces acting on the wall. As well as the inertia load w_{in}, there is the applied load P transmitted by walls and floors above, and the self weight W of the wall, divided into two equal parts W/2 centred above and below the central crack as shown. The resultant gravity force R acting on the upper half of the wall has the magnitude

$$R = P + \frac{W}{2} \qquad (7)$$

and acts at a distance

$$y_R = \frac{h_c}{4}\left[\frac{W}{2(P + \frac{W}{2})}\right] \qquad (8)$$

from the top of the wall.

At ultimate conditions, the compression zone at the central crack is as shown in Fig. 8b. The depth of the compression zone can be approximated as

$$a = \frac{R}{0.85 f'_m} \qquad (9)$$

and the resultant force R acts at distance a/2 from the inside of the wall.

Figure 8c shows the displaced shape of the upper portion of the wall at incipient instability, when the line of action of the resultant load and the compression force at the central crack are co-linear. Any further lateral displacement will result in an unstable situation, and failure will result. If the displacement at the wall centre is Δ_u, and the displacement at the centre of load is Δ', then conservatively approximating the displacement profile by a linear distribution,

$$\Delta' = \frac{2\,y_R}{h_c}.\Delta \qquad (10)$$

and for instability

$$\Delta_u - \Delta' = \frac{t - a}{2} \qquad (11)$$

where t is the wall thickness. Combining Eqns. 10 and 11,

$$\Delta_u = \frac{h_c(t - a)}{2(h_c - 2\,y_R)} \qquad (12)$$

Load-deflection relationship for wall

In order to assess the energy requirements at failure, it is necessary to develop the load-deflection relationship for the wall under face loading.

Prior to cracking, the response is linear elastic. Figure 9a shows the stress conditions at the central section when cracking is about to occur, assuming zero tension strength. Thus, taking moments of the resultant force about the wall centroid,

$$M_{cr} = \frac{Rt}{6} \tag{13}$$

and

$$f_{cr} = \frac{2R}{t} \tag{14}$$

where f_c is the maximum compresson stress. The lateral load required to cause M_{cr} will be given by

$$M_{cr} = \frac{w_{in} h_c^2}{8}$$

Hence (15)

$$w_{in} = \frac{8 M_{cr}}{h_c^2}$$

Since $w_{in} = m \ddot{a}_{in}$, the acceleration required to cause cracking can be readily calculated. The displacement at the centre of the wall is given by

$$\Delta_{cr} = \frac{5 w_{in} h_c^4}{384 EI} \tag{16}$$

where

$$I = \frac{t^3}{12} \tag{17}$$

is the moment of inertia for a unit width of wall. Figure 9b shows the stress distribution when the crack has propagated to the wall centroid. The resisting moment is now

$$M = \frac{Rt}{3} = 2 M_{cr} \tag{18}$$

At cracking, the curvature at the central section was

$$\psi_{cr} = \frac{f_{cr}}{Et} \tag{19}$$

For conditions represented by Fig. 9b, the curvature will be

$$\psi = \frac{2 f_{cr}}{E \, t/2} = 4 \psi_{cr} \tag{20}$$

It may conservatively be assumed that the displacement Δ increases in proportion with the central curvature. Thus, for the stress conditions of Fig. 9b, the central displacement will be

$$\Delta \doteqdot 4 \Delta_{cr} \tag{21}$$

A more accurate estimate for can be obtained by integrating the curvature distribution, but is probably not warranted when other approximations made in the analysis are considered. In fact, the errors are typically not large until very large displacements are obtained.

The lateral load w_{in} causing the moment is calculated as shown in Fig. 10. Taking moments about 0, on the wall centre line at the central section,

$$R.x = \frac{w_{in} h_c^2}{8} + R(\Delta - \Delta') \tag{22}$$

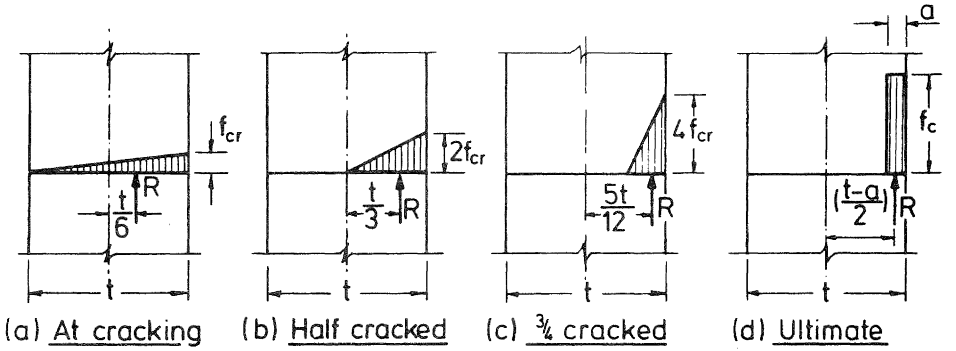

Figure 9. Moments and curvatures at centre of face-loaded wall.

where x is the distance between the line of action of R and the wall centre line (note x = t/3 for Fig. 9b). Thus

$$w_{in} = \frac{8}{h_c^2} R(x - (\Delta - \Delta')) \qquad (23)$$

Note that the wall deformation Δ reduces the magnitude of the lateral inertia load required to develop the moment R.x. That is, a P-Δ, or in this case an R-Δ effect exists. At the limit, when instability is incipient, $w_{in} = 0$. The response acceleration corresponding to w_{in} is

$$\ddot{a}_{in} = \frac{8}{m\, h_c^2} R(x - (\Delta - \Delta')) \qquad (24)$$

Using the procedure outlined above, the complete load-deflection, or acceleration-deflection curve can be calculated. Figure 9c shows the calculations for the situation when the crack has propagated to 3/4 of the section depth, and Fig. 9d shows conditions at ultimate. It should be noted that calculations will normally indicate that instability occurs before the ultimate stress conditions represented by Fig. 9d are reached. It should also be noted that the ultimate moment in Fig. 9d has a magnitude $M_u \leq 3M_{cr}$, where M_{cr} is the cracking moment, with the upper limit being approached only for very small axial loads R, since $a \to 0$.

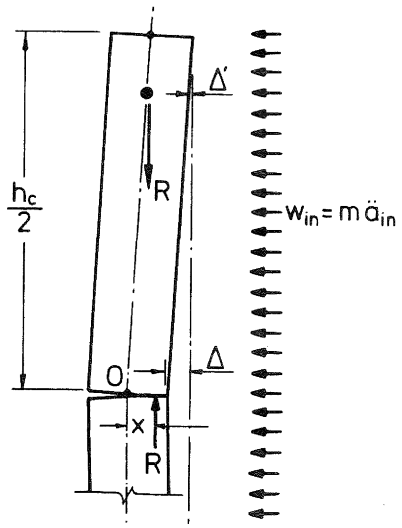

Moments at 0 :-

$$Rx = \frac{w_{in} h_c^2}{8} + R(\Delta - \Delta')$$

$$\therefore \ddot{a}_{in} = \frac{w_{in}}{m} = \frac{8}{m h_c^2} R(x - (\Delta - \Delta'))$$

Figure 10. Moment equilibrium for face-loaded wall.

The form of the acceleration-displacement curve is indicated by the curved line in Fig. 11. This curve is elastic non-linear. that is, the wall will 'unload' down the same curve. It is suggested that an estimate of the equivalent elastic response acceleration a_e can be found by the 'equal-energy' principle, equating an area under a linear acceleration-displacement line with the same initial stiffness k as the true wall acceleration-displacement curve, as shown in Fig. 11. If A_1 is the area under the true curve, then

$$A_2 = \frac{\ddot{a}_e^{\,2}}{2k} = A_1$$

hence

$$\ddot{a}_e = \sqrt{2 k A_1} \qquad (25)$$

is the equivalent elastic response acceleration to induce failure.

In calculating the response using the methodology outlined above, some account of vertical acceleration should be taken, since these reduce the moments required for a given acceleration. Conservatively, it is suggested that a value equal to 2/3 of the peak lateral ground acceleration should be adopted. An example of the use of the methodology for a five-storey unreinforced masonry building with perimeter walls is given in an Appendix to this paper. The results of this example indicate that, as expected, the top floor is the most critical, but that equivalent accelerations to induce failure are suprisingly high, given the conservative nature of the assumptions made.

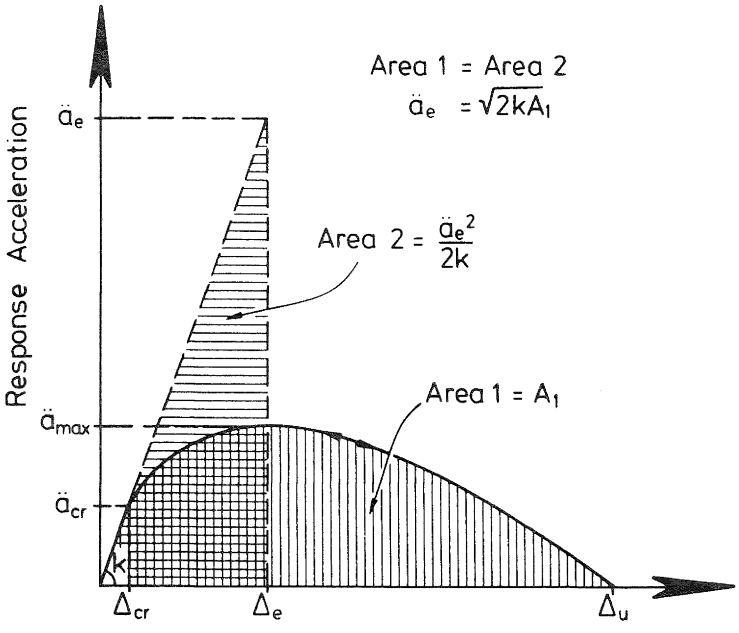

Figure 11. "Equal Energy" principle for equivalent elastic stiffness.

UNREINFORCED WALLS SUBJECTED TO IN-PLANE EXCITATION

The methodology developed above for estimating the level of earthquake excitation necessary to induce failure of a face-loaded wall can also be used for walls under in-plane loading. However, for large walls without openings, it will generally be found that no real instability will occur, and that the walls will simply rock on their bases. If the uplift displacements are too large, failure may occur gradually by shedding bricks from the tension end of the wall. Many unreinforced concrete structures subjected to seismic loading have shown signs of relative displacements at one or more levels. This can be attributed to rocking response with simultaneous accelerations in the face load direction.

The behaviour of walls with openings under in-plane loads requires deeper consideration, however.

Figure 12a illustrates a typical example of a wall divided into four piers by openings. Figure 12b and 12c represent maximum shear forces that can be transmitted by a typical pier in a rocking mode and shear failure mode respectively.

For the rocking mode, stability is provided by the axial load P. Taking moments about the toe reaction P, and ignoring the pier self weight as being insignificant,

$$P.(\ell_p - a) = V.h_o$$

i.e.
$$V = \frac{P(\ell_p - a)}{h_o} \qquad (26)$$

where
$$a = \frac{P}{0.85\ f'_m.t}$$

is the compression contact area at ultimate, and t is the wall thickness.

Very large displacements ($\Delta = \ell_p - a$) will be necessary to induce instability failure under the rocking mode. The analysis developed for face-loaded walls can be used to estimate maximum equivalent elastic response.

The shear force indicated by Eqn. 26 can only develop if shear failure of the pier does not occur at a lower shear force. From Fig. 12c, the shear failure load will be

$$V = \tau_o\ \ell_p.t + \mu P \qquad (27)$$

where τ_o is the initial shear stress for zero axial load, and μ is a friction coefficient. Testing of unreinforced masonry walls suggests appropriate values in the range

$$0.1 \leq \tau_o \leq 1.2\text{MPa}$$
$$0.5 \leq \mu \leq 1.2 \qquad (28)$$

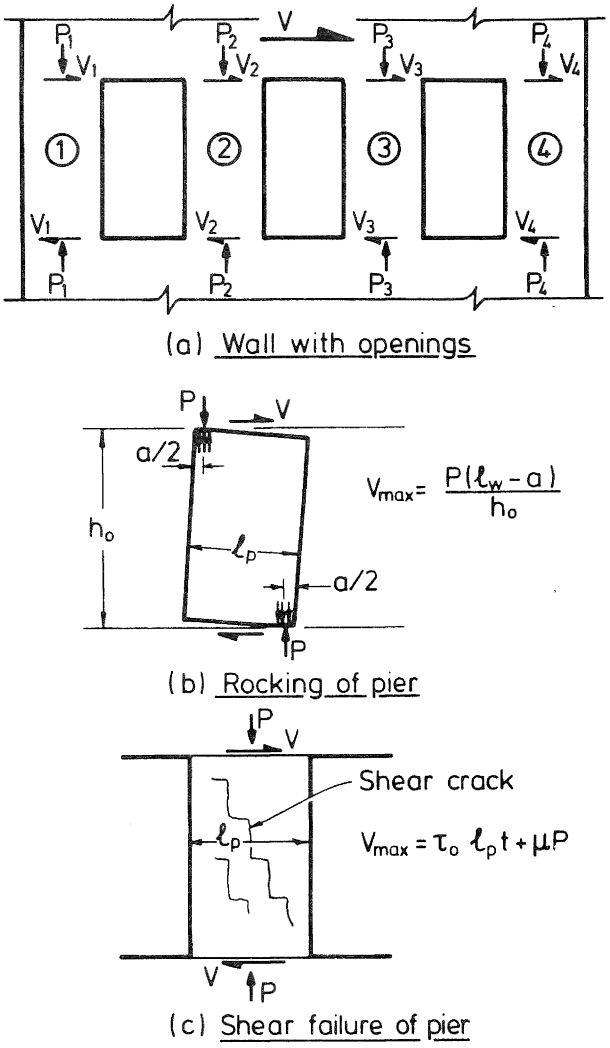

Figure 12. Failure of unreinforced wall with piers.

Equation 27 assumes that when incipient shear cracking develops, the shear stress is effectively uniformly distributed across the section, rather than distributed parabolically. In such circumstances, and considering the repeated load reversals expected under seismic loading, it is advisable to put $\tau_o = 0$. Hence

$$V = \mu P \qquad (29)$$

Equations 26, 27 and 29 can be combined to find the critical aspect ratio for piers, to ensure shear failure does not occur. Thus

$$\mu P > \frac{P}{h_o}\left(\ell_p - \frac{P}{0.85\ f'_m t}\right)$$

let
$$f_c = \frac{P}{\ell_p.t}$$

be the average axial compression stress on the pier. Then

$$\mu > \frac{\ell_p}{h_o}\left(1 - \frac{f_c}{0.85\ f'_m}\right)$$

or

$$\frac{h_o}{\ell_p} > \frac{1}{\mu}\left(1 - \frac{f_c}{0.85\ f'_m}\right) \qquad (30)$$

In the absence of information relating to the coefficient of friction for the wall being assessed it is recommended that $\mu = 0.5$ be adopted. Thus

$$\frac{h_o}{\ell_p} > 2\left(1 - \frac{f_c}{0.85\ f'_m}\right) \qquad (31)$$

is the requirement to avoid shear failure. Consequently piers with aspect ratios greater than 2.0 should not be subject to shear failure. For piers with heavy axial load, lower aspect ratios may be satisfactory, since these rock at a relatively lower shear.

It is recommended that the criterion of acceptable performance for piers be that shear failure cannot occur. Provided rocking limits the shear capacity of all piers at a given level, simple addition of the pier shear forces gives the total storey shear.

It should be noted that for face-loading, the influence of wall openings is to increase the axial load on the piers, thus making them more stable. This aspect can easily be incorporated in the methodology developed above.

CONCLUSIONS

Examination of working stress and ultimate strength methods for assessing unreinforced masonry strength under seismic loading indicated that neither method could give an adequate representation of the dynamic response. An ultimate load appraisal incorporating energy consideration based on the calculated load-deflection curves appears to have some merits for assessment of face-load response of masonry walls. In developing the methodology for analysis a number of conservative assumptions were made. The significance of these assumptions should be tested by dynamic analyses and testing, and where possible, by back-calibrating against results from earthquakes.

The analyses produced the not unexpected result that upper floors of masonry buildings are likely to be more suspect than lower floors, since accelerations will be higher, and stabilising moments provided by gravity loads will be less. The analyses assumed that the walls are properly connected to the floor (and roof) system at all levels. Generally this will not be the case. Fig. 13 shows a detail common in unreinforced masonry walls in New Zealand, where the floor beam rests on the wall in a small 'pocket'. Connection between wall and floor relies on friction. Because of the high accelerations possible, this is inadequate, and positive connection, preferably using anchor bolts connected to the floor beam and anchored against a bearing plate on the outside of the wall should be used. Examination of the methodology developed above for face-load response immediately shows the disasterous consequences of loosing support by connection to the roof or to an intermediate floor.

No attempt has been made in this paper to discuss methods for upgrading the seismic capacity of walls where face-load or in-plane shear capacity is shown to be inadequate. These have been adequately covered in recent issues of the Bulletin.

Finally it should be noted that comments presented in this paper assume good quality masonry properties, and would obviously not apply to walls with decayed mortar and loose bricks. For other structures, made from competent materials, the methodology would indicate that our assessment of the capacity of existing unreinforced masonry buildings may have been somewhat Draconian in the past, and that less conservative assessments and requirements for strengthening may often be appropriate. It is hoped that this paper may stimulate discussion of some of these aspects.

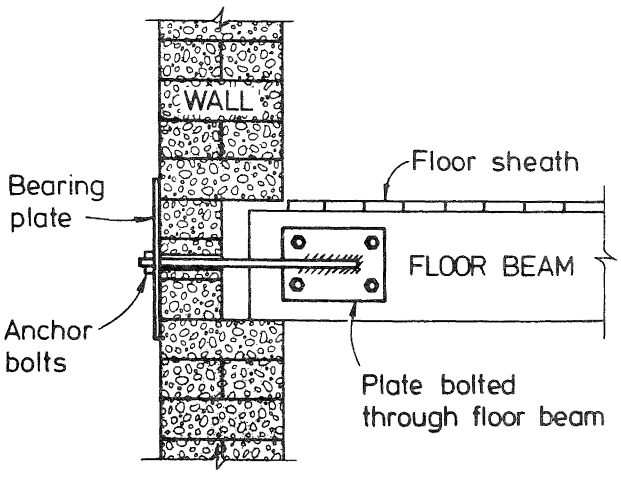

Figure 13. Anchoring floor beams to walls.

REFERENCES

(1) Priestley, M.J.N. (1980). "Seismic Design of Masonry Buildings - Background to the Draft Masonry Code." Bulletin NZNSEE 13 (4): 329-346.

(2) NZS 4230P:1985 "Code of Practice for the Design of Masonry Structures." Standards Ass. of New Zealand. Wellington. 130p.

(3) Kariotis, J.C., Ewing, R.D. and Johnson, A.W. (1985). "Predictions of Stability for Unreinforced Brick Masonry Walls Shaken by Earthquakes." Proc. 7th International Brick Masonry Conference. Melbourne. 2: 1175-1184.

(4) Kariotis, J.C., Ewing, R.D, Johnson, A.W. and Adham, S.A. (1985). "Methodology for Mitigation of Earthquake Hazards in Unreinforced Brick Masonry Buildings." Proc. 7th International Brick Masonry Conference. Melbourne. 2: 1339-1350.

(5) Priestley, M.J.N., Thorby, P.N., McLarin, M.W. and Bridgeman, D.O. (1979). "Dynamic Performance of Brick Masonry Veneer Panels." Bull. NZNSEE 12 (4): 314-323.

APPENDIX

Example of Unreinforced Masonry Building Response

The five-storey unreinforced masonry building in Fig. 14a has perimeter walls 220 mm thick. The 20 m long end walls support masses of 40 tonnes per floor (including self weight) and 20 tonnes at roof level. Use the design elastic response spectrum of Fig. 14b to estimate the natural in-plane period of the end walls, and hence the wall response accelerations. Assuming that flexible floors amplify the end wall accelerations by a factor of 2.0, calculate at what proportion of the design loading failure of a longitudinal face-loaded wall (see Fig. 14a) would occur at levels 5, 3 and 1, assuming load applied to the wall by the roof is 10 kN/m, and load applied by each floor is 14 kN/m (self weight must be added).

Data:

Elastic Modulus:

$$E = 1.0 \text{ GPa}$$

Shear Modulus:

$$G = 0.4 \text{ GPa}$$

Brick Density $= 1900 \text{ kg/m}^3$

Masonry comp. strength:

$$f'_m = 5 \text{ MPa}$$

Foundation rotational stiffness:

$$k_\theta = 8.5 \times 10^9 \text{ Nm/radian}$$

Vertical accelerations:
Assume 0.2 g in conjunction with horizontal acceleration (= 2/3 of peak ground horizontal acceleration).

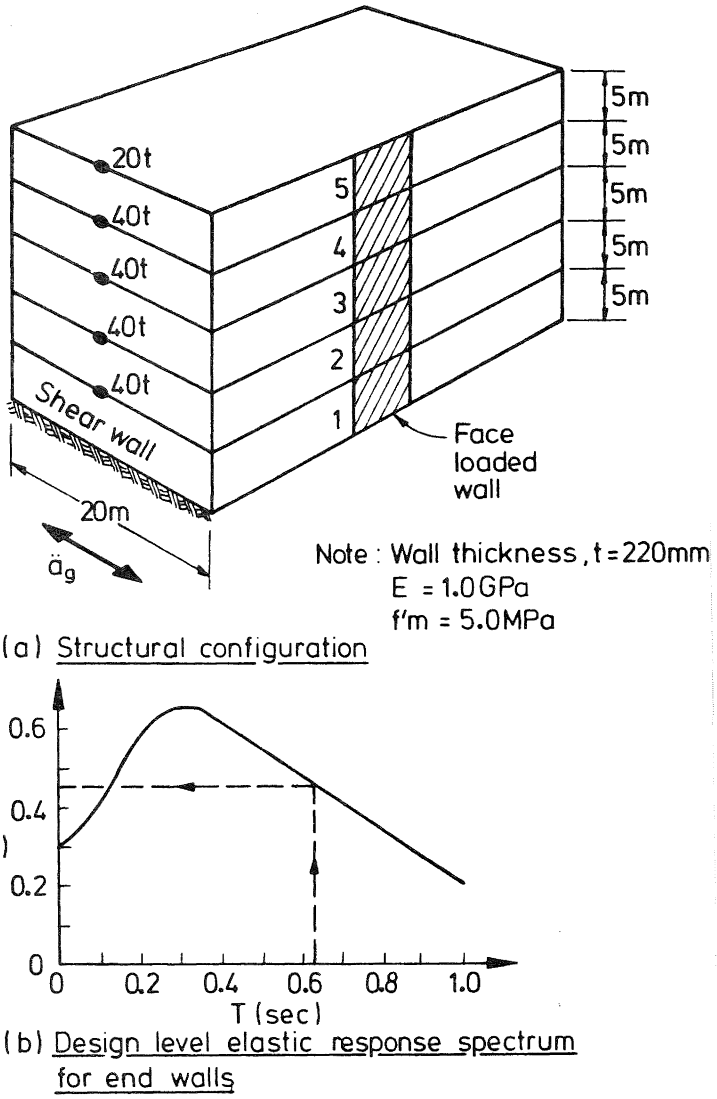

Figure 14. Design example for 5 storey masonry building.

Solution:

In-plane response of end wall

Moment of inertia:

$$I = \frac{0.22 \times 20^3}{12} = 146.7 \text{ m}^4$$

Natural period: For the equivalent 1^oF model

$$T = 2\pi\sqrt{\frac{m_e}{k_e}}$$

$$= 2\pi\sqrt{\frac{180 \times 10^3}{1.76 \times 10^7}} \text{ sec.}$$

i.e. $T = 0.635$ sec.

From Fig. 14b, the response acceleration at the centre of mass = 0.44 g where g = acceleration due to gravity.

Moment to cause in-place rocking

Check stability under 0.8D + E (D = dead load, E = earthquake load).

Restoring moment:

$$M_r = 0.8(180 \times 9.8(\frac{\ell_w}{2} - \frac{a}{2}))\ \text{kNm}$$

$$= 1.41(\frac{\ell_w}{2} - \frac{a}{2})\ \text{MNm}$$

$$a = \frac{0.8\ P_e}{0.85\ f'_m t}$$

$$= \frac{0.8 \times 180 \times 9.8}{0.85 \times 5000 \times 0.22}$$

$$= 1.51\ \text{m}$$

$$M_r = 1.41(\frac{20}{2} - \frac{1.51}{2})$$

$$= \underline{13.1\ \text{MNm}}$$

Overturning moment

At 0.44 g response:

$$M_o = 180 \times 0.44 \times 9.8 \times 17$$

$$= \underline{13.20\ \text{MNm}}$$

Thus the wall starts to rock at

$\frac{13.1}{13.2} \times 100 = 99\%$ of the design earthquake.

Design level floor accelerations

Area:

$$A = 0.22 \times 20 = 4.4\ \text{m}^2$$

Equivalent Single Degree of Freedom Model

A simple simulation of the transverse response of the shear walls can be provided by a single mass m_e at equivalent height h_e given by

$$m_e = \sum_1^5 m_i$$

$$= 4 \times 40 + 20$$

i.e. $m_e = \underline{180\ \text{tonnes}}$

and

$$h_e = \frac{\Sigma\ m_i\ h_i^2}{\Sigma\ m_i\ h_i}$$

$$= \frac{20 \times 25^2 + 40(20^2 + 15^2 + 10^2 + 5^2)}{20 \times 25 + 40(20 + 15 + 10 + 5)}\ \text{m}$$

i.e.

$h_e = \underline{17.0\ \text{m}}$

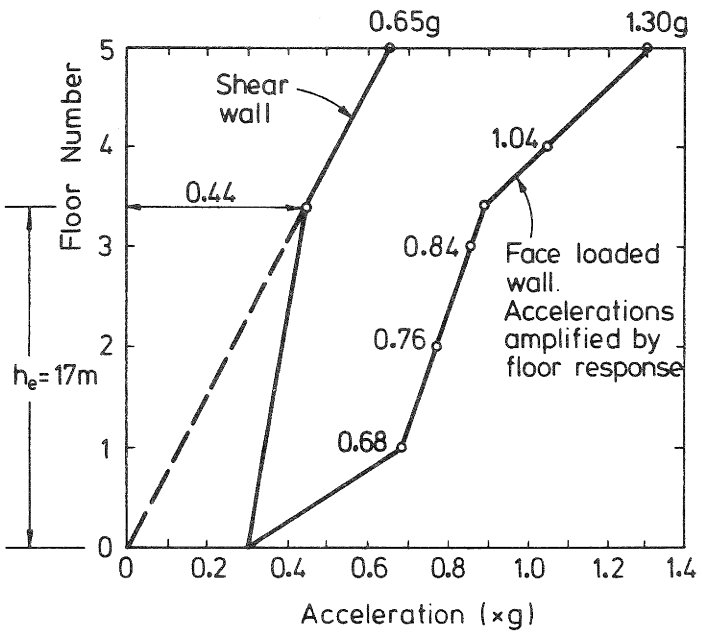

Figure 15. Response accelerations for example building.

Stiffness of Wall

The wall stiffness depends on the flexural, shear and foundation flexibility, and can be expressed as

$$k_e = \frac{1}{\left[\frac{h_e^3}{3EI} + \frac{1.2h_e}{AG} + \frac{h_e^2}{k_\theta}\right]}$$

$$= \frac{1}{\left[\frac{17^3}{3 \times 10^9 \times 146.7} + \frac{1.2 \times 17}{4.4 \times 0.4 \times 10^9} + \frac{17^2}{8.5 \times 10^9}\right]}$$

i.e. $k_e = \underline{1.76 \times 10^7\ \text{N/m}}$

Figure 15 shows the design-level shear wall accelerations at different heights, and the input accelerations for the face-loaded wall, which are 2.0 times the shear wall accelerations, except at ground floor level, where no amplification will occur.

5th storey face-load response

Referring to Fig. 8,

P = 0.8 x 10 kN = 8kN/m, and

W = 0.8 x 1.9 x 9.8 x 0.22 x 5 kN

= 16.4 kN/m

R = 8 + 8.2 = 16.2 kN/m

Note that the 0.8 factor is to allow for vertical acceleration of 0.2 g.

From Eqn. 8:

$$y_R = \frac{2.5}{2}\left(\frac{8.2}{16.2}\right)$$

$$= 0.629 \text{ m}$$

at cracking:

$$f_{cr} = \frac{2 \times 16.2}{0.22} = 0.147 \text{ MPa}$$

Eqn. 13:

$$M_{cr} = \frac{16.2 \times 0.22}{6} \text{ kNm}$$

$$= 0.595 \text{ kNm}$$

Eqn. 15: Equivalent lateral load

$$w_{in} = \frac{8 \times 0.595}{25}$$

$$= 190 \text{ N/m}$$

Eqn. 16: Central displacement

$$\Delta = \frac{5 \times 190 \times 5^4}{384 \times 10^9 \times \frac{0.22^3}{12}} \text{ m}$$

$$= 1.74 \text{ mm}$$

Eqn. 19: Curvature

$$\psi_{cr} = \frac{0.147}{10^3 \times 0.22} = 0.662 \times 10^{-3}/\text{m}$$

Now unit weight of wall

$$= 1.9 \times 9.8 \times 2.2 = 4.10 \text{ kN/m}^2$$

Thus from Eqns. 10 and 24 the true acceleration for a displacement of 1.74 mm will be

$$\ddot{a}_{in} = \frac{8}{4.10 \times 25} \times 16.2\left\{\frac{0.22}{6} - (1 - \frac{0.629}{2.5})0.00174\right\}$$

$$= 0.0447 \text{ g}$$

Thus the top level wall will crack at the very low response acceleration of 0.0447 g.

For a moment $M = 2\ M_{cr}$ (e.g. Fig. 9b)

we have $\psi = 4\ \psi_{cr} = 2.64 \times 10^{-3}/\text{m}$

and $\Delta = 4 \times 1.74$ mm

$= 6.96$ mm

The corresponding acceleration will be

$$\ddot{a}_{in} = \frac{8}{4.10 \times 25} \times 16.2\left\{\frac{0.22}{3} - (1 - 0.25)0.00696\right\}$$

$$= 0.0861 \text{ g}$$

For a moment $M = 2.5\ M_{cr}$ (e.g. Fig. 9c)

$$\psi = 16\ \psi_{cr} = 10.56 \times 10^{-3}/\text{m}$$

$$\Delta = 16\ \Delta_{cr} = 27.84 \text{ mm}$$

$$\ddot{a}_{in} = 1.26(0.0917 - 0.75 \times 0.02784)\ g$$

$$= 0.0892 \text{ g}$$

For a moment $M = 2.667\ M_{cr}$ ($f_c = 6\ f_{cr}$)

$$\psi = 36\ \psi_{cr} = 23.8 \times 10^{-3}/\text{m}$$

$$\Delta = 36\ \Delta_{cr} = 62.6 \text{ mm}$$

$$\ddot{a}_{in} = 1.26(0.0978 - 0.75 \times 0.0626)\ g$$

$$= 0.0644 \text{ g}$$

The moment-curvature and acceleration-displacement curves for level 5 are included in Figs. 16 and 17 respectively. These figures also include curves for level 3 and level 1 based on similar calculations to the above, but with axial load levels of

Level 3: $R = 0.8 \times 89.3 = 71.4$ kN/m

Level 1: $R = 0.8 \times 158.3 = 126.6$ kN/m

The increased load greatly improves the moment-curvature behaviour, but because of the greater P-Δ effect on central moments, the acceleration:displacement curves are not enhanced to the same degree.

The areas under the three acceleration: displacement curves can be measured to give

Level 5: $A_5 = 7.25$ (mm x g units)

Level 3: $A_3 = 14.8$ (mm x g units)

Level 1: $A_1 = 14.8$ (mm x g units)

The initial stiffness of all three curves is the same, at

$$k = 0.0259 \text{ g/mm}$$

Thus the equivalent elastic response acceleration to induce failure can be calculated using Eqn. 25.

Level 5: $\ddot{a}_e = \sqrt{2\ kA_5}\ g$

$$= \sqrt{2 \times 0.0259 \times 7.25}\ g$$

$$= 0.61 \text{ g}$$

Level 3 and 1:

$$\ddot{a}_e = \sqrt{2 \times 0.0259 \times 14.8}\ g$$

$$= 0.875 \text{ g}$$

These can be compared with the response accelerations corresponding to the design level earthquake, given in Fig. 15. For level 5, the average acceleration is

$$\ddot{a} = \frac{1.04 + 1.30}{2}$$

$$= 1.17 \text{ g}$$

Hence failure of the Level 5 wall is expected at

$$\frac{0.61}{1.17} \times 100\% = 52\%$$

of the design level earthquake.

Design level accelerations for levels 3 and 1 are 0.80 g and 0.49 g respectively. Consequently failure at three levels will not occur until 109 percent and 179 percent respectively of the design level earthquake. However, premature failure of the level 5 wall could induce failures at lower levels, due to reduced stability moments, and possible loss of floor support.

As expected, these calculations show the top level of the wall to be most vulnerable to damage from face-load accelerations. Although the calculations can only be considered approximate, the general conclusions are valid, and the methodology sound. In particular the analyses indicate the sensitivity of the results to simultaneous vertical acceleration. For levels of vertical acceleration higher than the 0.2 g assumed in this example, the failure lateral accelerations will be correspondingly lower.

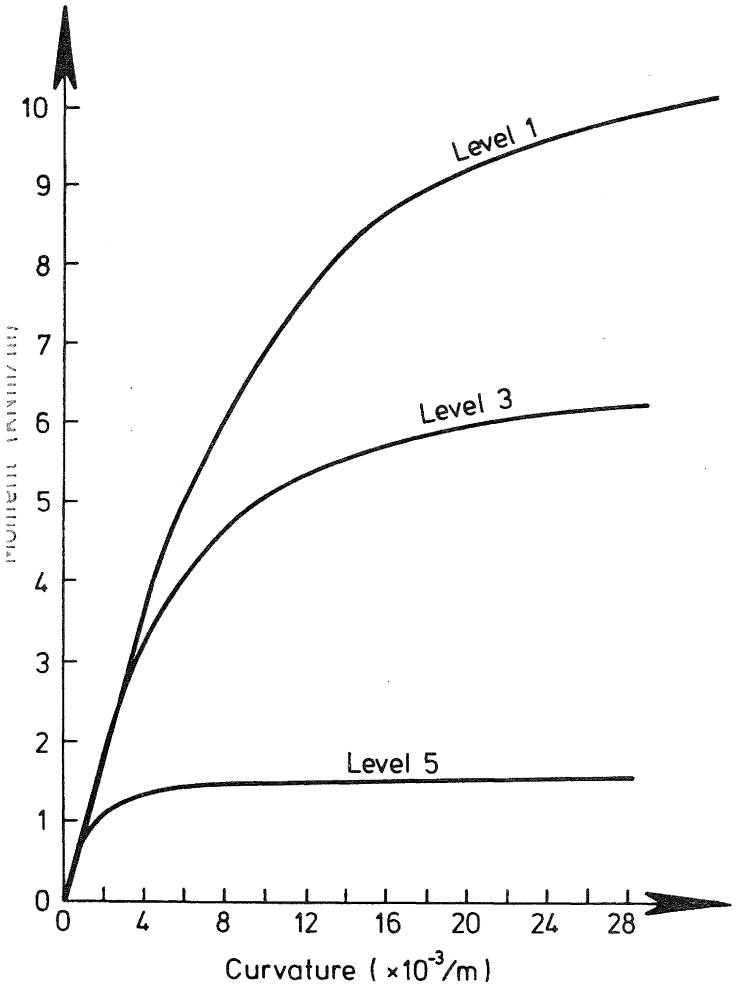

Figure 16. Moment-curvature relationships for face-loading at different levels for example building.

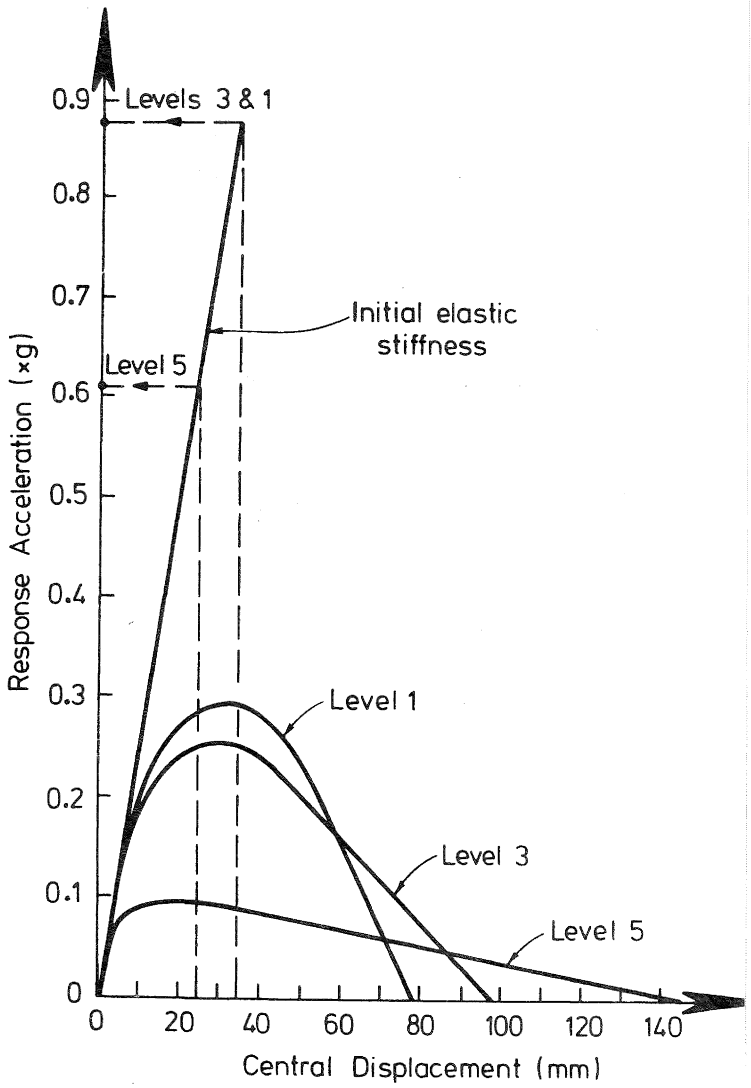

Figure 17. Equivalent elastic response accelerations at different levels for example building.